# Spectral element schemes for high order partial differential equations : Application to the Korteweg-de Vries model

Sebastian Minjeaud, Richard Pasquetti

# SPECTRAL ELEMENT SCHEMES FOR HIGH ORDER PARTIAL DIFFERENTIAL EQUATIONS : APPLICATION TO THE KORTEWEG-DE VRIES MODEL *

SEBASTIAN MINJEAUD AND RICHARD PASQUETTI †

**Abstract.** We address the Korteweg-de Vries equation as an interesting model of high order partial differential equation, and show that using the classical spectral element method, *i.e.* a high order continuous Galerkin approximation, it is possible to develop satisfactory schemes, in terms of accuracy, computational efficiency, simplicity of implementation and, if required, conservation of the lower invariants. The proposed approach is *a priori* easily extensible to other partial differential equations and to multidimensional problems.

**Key words.** Spectral element method; IMEX schemes; Stabilization techniques; invariants conservation; KdV equation.

**AMS subject classifications.** 65M60, 65M70, 65L06.

**1. Introduction.** As now well known, the spectral element method (SEM) allows a high order approximation of partial differential equations (PDE) and combines the advantages of spectral methods, that is accuracy and rapid convergence, with those of the finite element method (FEM), that is geometrical flexibility. Since the pioneering work of [33], which was based on interpolation using Chebyshev polynomials, several important developments of the method have been achieved. The spectral element schemes that we introduce in this paper rely, say, on the "standard" SEM, see *e.g.* [11, 16, 24, 28].

The SEM is based on a nodal continuous Galerkin (CG) approach, such that the approximation space contains all $C^0$ functions whose restriction in each element is a polynomial of degree $N$. In each element the basis functions are Lagrange polynomials associated to the Gauss-Lobatto-Legendre (GLL) points and these GLL interpolation points are also used as quadrature points to evaluate integrals derived using a weak form of the problem. An important consequence is that the resulting mass matrix is diagonal, so that for evolution problems the SEM is particularly attractive if used in conjunction with explicit time-stepping schemes. This is the reason why the same approach is sometimes called "Gauss-point mass lumped finite element scheme" in the finite element literature [14].

The efficiency of the SEM is definitely proven for the elliptic or parabolic PDEs, whose solutions are in general smooth. However, severe stability problems have also been encountered in the past, especially when dealing with hyperbolic PDEs, since, roughly speaking, spectral approximations are much less numerically diffusive than low-order ones. When shocks occur, the SEM has to be stabilized. Among the stabilization techniques well adapted to the SEM approximation, one can cite the variational multiscale method [21], the entropy viscosity method [19] or the spectral vanishing viscosity (SVV) technique [37].

*This study was supported by the EUROFUSION project "Synergetic numerical-experimental approach to fundamental aspects of turbulent transport in the tokamak edge". We also thank our Colleagues D. Clamond and A. Galligo for fruitful discussions.

†Lab. J. A. Dieudonné, UMR CNRS 7351, Université de Nice-Sophia Antipolis, F-06108 Nice, France & INRIA project CASTOR. (minjeaud/pasquetti@unice.fr). Questions, comments, or corrections to this document may be directed to that email address.

Applying the SEM to dispersive problems, *e.g.* third or higher odd-order equations, is however not trivial. As a relevant example of such problems we consider the Korteweg-de Vries (KdV) equation, which is well known to point out the dispersive effects that may occur for weakly non-linear water waves or collisionless plasmas, and to provide a simple evidence of the existence of solitons, see *e.g.* [30] and references herein. With $t \in \mathbb{R}^+$ and $x \in \Omega = (x_{\min}, x_{\max})$ for the time and space variables, the KdV PDE may write:

$$\partial_t u + u\partial_x u + \beta \partial_{xxx} u = 0\,, \tag{1.1}$$

and should be completed with an initial condition $u_0 = u(x,0)$, $x \in \Omega$, and *e.g.* periodic boundary conditions. Many numerical methods have been proposed and implemented to compute approximate solutions of (1.1). The existing techniques include finite-difference methods [35, 42], spectral methods [36], finite-element methods [4, 6, 34, 41], and more recently finite volume methods [17] or discontinuous Galerkin methods [40]. In the frame of FEMs, third (or higher) order derivative terms raise some difficulties. When thinking to the standard $P_1$ finite element method, *i.e.* when using a piecewise linear approximation, it is indeed clear that the second order derivative vanishes in each element, so that it is *e.g.* required to use $C^1$ continuous finite elements or a Petrov-Galerkin approach with $C^1$ test functions, but at the price of an additional complexity of the algorithm especially when one has in mind high order approximations or multi-dimensional problems. In this article, we want to show that a high order approximation can be obtained on the basis of $C^0$ finite elements and propose approaches that remain simple to implement.

This paper is organized as follows. In Section 2 we first discuss the time discretization for the KdV problem and then address the space discretization, on the basis of the SEM approximation. Two different variants are introduced to handle the third order derivative term: the first one may be considered as the most natural to avoid using $C^1$ finite elements whereas the second one is the most general to approximate high order derivative terms with $C^0$ finite elements. We then consider, in Section 3, the non-linear transport term, and discuss two possibilities of numerical stabilization, on the basis of the overintegration of this non-linear term and/or by using the spectral vanishing viscosity technique. The preservation of the lower invariants of the KdV equation is discussed in Section 4. Finally, in Section 5, we experiment the different schemes.

## 2. Discretization.

**2.1. Time discretization.** For the sake of computational efficiency, we propose to handle the non-linear term $\mathcal{N}(u) = u\partial_x u$ explicitly, whereas for the sake of numerical stability, we propose an implicit treatment of the linear term $\mathcal{L}(u) = \beta\partial_{xxx}u$. Moreover, with this choice, one can expect the usual Courant-Friedrichs-Lewy (CFL) stability condition.

To obtain a high order approximation in coherence with the SEM, we propose to use an implicit-explicit (IMEX) Runge Kutta (RK) scheme. The IMEX schemes were first developed in the 90's [2] and details may now be found in several papers, see *e.g.* [32]. They combine an Explicit RK (ERK) scheme for the operator $\mathcal{N}$ and an Implicit RK (IRK) scheme for the operator $\mathcal{L}$. Denoting by $\tau$ the time step, a

$s$-stages IMEX scheme for the ODE $\partial_t u = \mathcal{N}(u) + \mathcal{L}(u)$, may read as follows

$$\begin{cases} u_{n,i} = u_n + \tau \sum_{j=1}^{s} \Big( \hat{a}_{ij} \mathcal{N}_j + a_{ij} \mathcal{L}_j \Big), \quad \forall i = 1, .., s, \\ u_{n+1} = u_n + \tau \sum_{j=1}^{s} \Big( \hat{b}_j \mathcal{N}_j + b_j \mathcal{L}_j \Big). \end{cases}$$

where the $\mathcal{N}_j \equiv \mathcal{N}(u_{n,j})$ and $\mathcal{L}_j \equiv \mathcal{L}(u_{n,j})$ are the values of $\mathcal{N}(u)$ and $\mathcal{L}(u)$ at the intermediate RK steps. The two schemes are defined by the coefficients $\hat{A} = (\hat{a}_{ij})$, $\hat{b} = (\hat{b}_j)$ and $A = (a_{ij})$, $b = (b_j)$, $1 \leqslant i, j \leqslant s$, which are classically gathered in a Butcher tableau, see *e.g.* [8]. The coefficients in $\hat{A}$ should vanish when $j \geqslant i$ since they define an explicit scheme. Concerning the implicit part, IMEX schemes generally make use of Diagonally IRK (DIRK) schemes, that is $a_{ij} = 0$ if $j > i$. Consequently, the intermediate unknowns $u_{n,i}$ can be successively computed by "inverting" the operators $Id - \tau a_{ii} \mathcal{L}$, for $i = 1, .., s$ ($Id$, for identity operator). Moreover, it is usual to assume that the normalized intermediate times $c_i = \sum_{j=1}^{s} a_{ij} = \sum_{j=1}^{s} \hat{a}_{ij}$ of the two schemes coincide and also the coefficients in $\hat{b}$ and $b$ are often the same (in that case, the order of the resulting IMEX scheme is exactly the minimum of the order of its two constituting schemes).

An IMEX scheme preserves all the linear invariants but, as an ERK scheme, it cannot preserve all the quadratic invariants. However, it is possible to focus on a specific quadratic invariant and ensure its conservation (see Section 4).

In this article, we mainly use the IMEX scheme ARS (2,3,3) [3], characterized by 2 implicit steps, 3 explicit ones and which is globally third order accurate. Using Butcher's like notation, the coefficients of ARS(2,3,3) are provided in Table 2.1, where $\gamma = (3 + \sqrt{3})/6$.

| $c$ | $\hat{A}$ | $A$ | $\longleftrightarrow$ | 0 | 0 | 0 | 0 | 0 | 0 | 0 |
|---|---|---|---|---|---|---|---|---|---|---|
| | | | | $\gamma$ | $\gamma$ | 0 | 0 | 0 | $\gamma$ | 0 |
| | | | | 1 - $\gamma$ | $\gamma$ -1 | 2(1-$\gamma$) | 0 | 0 | 1-2$\gamma$ | $\gamma$ |
| | $\hat{b}$ | $b$ | | | 0 | 1/2 | 1/2 | 0 | 1/2 | 1/2 |

TABLE 2.1

*IMEX coefficients for ARS(2,3,3). The ERK scheme is defined at left of the vertical double bar and the DIRK scheme at right . The normalized intermediate times $c_i$ are given in left column.*

**2.2. Space discretization.** As explained in the introduction, the space discretization is based on the SEM so that the solution is sought in the space $E_h$ of all $C^0$ functions whose restriction in each element is a polynomial of degree $N$. Basically, the scheme is obtained using a weak formulation against test functions belonging to $E_h$. When considering a third (or higher) order term, the approximation space $E_h$ is not embedded in the Sobolev space $H^2$ (with usual notation), so that in the weak formulation nor the solution neither the test functions can accept two space derivatives. The basic idea we exploit to overcome this difficulty consists in introducing additional unknowns (belonging to $E_h$) which represent, in some sense, the first or second derivative of the solution, thus allowing to decrease the differential order in the weak formulation. Such an idea was already investigated for the KdV PDE, see

*e.g.* [20, 41]. But with the SEM, the key point lies in the fact that the intermediate unknowns can be *a posteriori* eliminated since the mass matrix is diagonal. Hence the method we propose does not suffer from an increase of the number of unknowns. Hereafter we describe two variants of the method and possible extensions.

We consider the following toy PDE to explain the space discretization of the third order term

$$\partial_t u + \beta \partial_{xxx} u = 0\,. \tag{2.1}$$

*Variant 1.* The most natural idea consists in introducing $f = \partial_{xx} u$ so that, instead of (2.1), we address the system

$$\begin{aligned} &\partial_t u + \beta \partial_x f = 0, \\ &f = \partial_{xx} u. \end{aligned}$$

This system can now be handled by the CG approach and the semi-discrete problem writes: find $(u_h, f_h) \in E_h \times E_h$ such that

$$\int_{x_{\min}}^{x_{\max}} \partial_t u_h v_h dx + \beta \int_{x_{\min}}^{x_{\max}} \partial_x f_h v_h dx = 0\,, \quad \forall v_h \in E_h\,, \tag{2.2}$$

$$\int_{x_{\min}}^{x_{\max}} f_h v_h dx + \int_{x_{\min}}^{x_{\max}} \partial_x u_h \partial_x v_h dx = 0\,, \quad \forall v_h \in E_h\,. \tag{2.3}$$

Note that here we consider periodic boundary conditions but (non-homogeneous) Neumann boundary conditions could be easily enforced by adding a boundary term in (2.3).

In algebraic form, one should then consider the system:

$$\begin{aligned} &M\partial_t U + \beta D F = 0, \\ &MF + BU = 0. \end{aligned}$$

The mass matrix $M$ and the matrices $D$ and $B$ write:

$$M_{ij} = \int_{x_{\min}}^{x_{\max}} \varphi_i \varphi_j \, dx\,, \quad D_{ij} = \int_{x_{\min}}^{x_{\max}} \varphi_i \partial_x \varphi_j \, dx\,, \quad B_{ij} = \int_{x_{\min}}^{x_{\max}} \partial_x \varphi_i \partial_x \varphi_j \, dx$$

where the set $\{\varphi_i\}$ stand for the usual SEM basis, *i.e.*, in each element, the set of Lagrange polynomials associated to the GLL points. One can eliminate $F = -M^{-1}BU$ to obtain the expression

$$M\partial_t U - \beta D M^{-1} B U = 0,$$

which points out the matrix implementation, in the present CG approach, of the third order derivative term

$$A_1 = -DM^{-1}B.$$

In the general finite element framework, it could be intricate to compute this matrix since it requires to compute the inverse of the mass matrix. However, the SEM mass matrix $M$ is diagonal and setting up the operator $DM^{-1}B$ is then quite easy.

*Variant 2.* Another approach is to define, for any function $u_h \in E_h$, an approximation $u'_h \in E_h$ of its derivative $\partial_x u_h$ by $L^2$ projection. On the basis of the following problem: Given $u_h \in E_h$, find $u'_h \in E_h$ such that,

$$\int_{x_{\min}}^{x_{\max}} u'_h v_h \, dx = \int_{x_{\min}}^{x_{\max}} \partial_x u_h \, v_h \, dx \, , \quad \forall v_h \in E_h \, ,$$

one can define a differentiation operator which then can be used to approximate high order derivative terms. Again, this is especially simple when the SEM is concerned, because the SEM matrix is diagonal so that the previous mass matrix problem can be trivially solved. Using the notations introduced previously, one obtains the algebraic expression:

$$MU' = DU \, .$$

Such an approach clearly show a way to approximate higher derivative order terms: a matrix implementation of derivatives of order $p$ could be $D(M^{-1}D)^{p-1}$. For the equation (2.1), this approach immediately leads to an expression of a third order derivative algebraic operator

$$A_2 = D(M^{-1}D)^2 \, .$$

Since here we assume periodicity, an integration by parts clearly shows that the matrix $D$ is antisymmetric $D = -D^t$, and we find the following strictly equivalent expression of $A_2$

$$A_2 = -DM^{-1}D^tM^{-1}D \, .$$

This second expression may be of interest in a non periodic domain, to enforce an homogeneous Neumann condition (a boundary term arises if the condition is not homogeneous).

Coming back to the approximation of $f = \partial_{xx} u$, one has $MF = -D^tM^{-1}DU$, which is directly comparable to the usual weak form, used in the first variant, $MF = -BU$. The advantage of the first procedure is that matrix $B$ can be set up by assembling elementary matrices, contrarily to the algebraic operator that we have introduced. Note however that the band structure is preserved.

The proposed approach is equivalent to consider the problem: Find $u_h$, $f_h$ and $g_h$, in $E_h$ such that (2.2) holds and that:

$$\int_{x_{\min}}^{x_{\max}} f_h v_h dx = -\int_{x_{\min}}^{x_{\max}} g_h \partial_x v_h dx \, , \quad \forall v_h \in E_h \, , \tag{2.4}$$

$$\int_{x_{\min}}^{x_{\max}} g_h v_h dx = \int_{x_{\min}}^{x_{\max}} \partial_x u_h v_h dx \, , \quad \forall v_h \in E_h \, . \tag{2.5}$$

Here it should be mentioned that *variant 2* opens a way the exact conservation of the discrete energy. This can be proved by choosing $v_h = u_h$ in (2.2), $v_h = g_h$ in (2.4) and $v_h = f_h$ in (2.5), yielding, if the time derivative is exactly computed:

$$\frac{1}{2} \int_{x_{\min}}^{x_{\max}} \partial_t u_h^2 \, dx = \beta \int_{x_{\min}}^{x_{\max}} g_h \partial_x g_h \, dx = \frac{\beta}{2} [g_h^2]_{x_{\min}}^{x_{\max}} = 0$$

by periodicity. Note that the second equality results from the fact that, in the SEM frame, the computation of the space derivative and of the quadrature are here exact

(recall that GLL quadratures are exact for polynomials of degree $2N-1$). The result can also be derived from the algebraic system. Indeed, since the matrix $A_2$ is antisymmetric, when using the *variant 2* we have:

$$\langle A_2 U, U\rangle = 0 \Rightarrow \partial_t \langle MU, U\rangle = 0\,.$$

**3. Stabilization techniques.** It is known that the solution of KdV is smooth, provided that the initial data is smooth, and so that the third order derivative term provides a regularization, see *e.g.* [23]. However, some stabilization techniques can be needed to avoid some spurious oscillations in the numerical simulation, especially when the number of grid points becomes insufficient. Two stabilization methods have been investigated: (i) Overintegration of the non-linear term and (ii) spectral vanishing viscosity technique. The former is rather natural since a quadratic term is present. Nearly all the results presented in Section 5 have been obtained with exact integration of the non-linear term. The SVV stabilization can be also of interest since this technique is known to be efficient, in the frame of spectral methods, for the inviscid Burgers equation which can be formally obtained from the KdV equation in the limit $\beta = 0$. Nevertheless, even if this discussion is beyond the scope of the present paper, it is important to mention that the use of a viscous stabilization may be criticized since it is known [27] (see also [20]) that diffusive and dispersive regularizations of the inviscid Burgers equation lead to different solutions when the regularization parameter tends to 0.

*Overintegration.* In view of stabilization, the overintegration of the non linear terms (the transport term in the KdV equation) may be efficient [25, 31]. In the frame of the SEM, this can be achieved simply by

- introducing a finer grid, *e.g.* the GLL grid associated to the polynomial degree $M > N$,
- setting up an extension operator from the initial GLL grid to the finer one,
- carrying out the integration of the concerned terms on the fine grid.

Thus, for KdV we first extend $u_h$ and $\partial_x u_h$ on the finer grid and then use the GLL quadrature associated to this finer grid to compute the integral of $v_h u_h \partial_x u_h$, where $v_h$ is again the test function. Exact integration can be obtained with $M$ such that $2M-1 \geq 3N-1$, *i.e.* $M \geq 3N/2$. However, as outlined, in [25, 31], for stabilization purposes using $M = N+1$ or $M = N+2$ may be sufficient.

*SVV stabilization.* The spectral vanishing viscosity (SVV) technique, as introduced in [29, 37] for the Fourier and Legendre spectral approximations of the Burgers equation, is a viscous stabilization in spectral space. It is controlled by two parameters, say $m_N$ and $\epsilon_N$, which define the threshold and the magnitude of this additional viscous term and that depend on the polynomial approximation degree $N$. In the frame of the SEM it is relevant to consider the stabilization term, in the reference interval $(-1,1)$

$$S_N = \epsilon_N \partial_x Q_N(\partial_x u_N)$$

where we denote by $u_N$ the polynomial approximation of degree $N$ and by $Q_N$ the spectral viscosity operator such that, for any polynomial $v_N \in \mathbb{P}_N(-1,1)$,

$$Q_N(v_N) = \sum_k \hat{Q}_k \hat{v}_k L_k(x)\,.$$

The $\hat{v}_k$ are the components of $v_N$ in the (orthogonal and hierarchical) Legendre basis $\{L_k\}$, and the $\hat{Q}_k$ are monotonically increasing coefficients such that, $\hat{Q}_k = 0$ if

$k \leq m_N$ and $0 < \hat{Q}_k \leq 1$ otherwise. As suggested in [29], we use $\hat{Q}_k = \exp(-(k-N)^2/(k-m_N)^2)$ for $m_N < k \leq N$.

Using now $v_N$ as a test function, in weak form the stabilization term writes (boundary terms are neglected):

$$\begin{aligned}\int_{-1}^{1} v_N S_N \, dx &= \epsilon_N \int_{-1}^{1} v_N \partial_x Q_N(\partial_x u_N) \, dx \\ &= -\epsilon_N \int_{-1}^{1} \partial_x v_N Q_N(\partial_x u_N) \, dx \\ &= -\epsilon_N \int_{-1}^{1} Q_N^{1/2}(\partial_x v_N) Q_N^{1/2}(\partial_x u_N) \, dx\end{aligned}$$

where in the last equality, which results from the orthogonality of the Legendre polynomials, $Q_N^{1/2}$ is defined as $Q_N$, but using the coefficients $\sqrt{Q_k}$. This last form is especially of interest when multidimensional SEM approximations are considered [39], whereas in the frame of the 1D SEM used in this paper, the two forms are strictly equivalent.

**4. Preservation of invariants.** As *e.g.* explained in [18], the KdV equation is characterized by an infinity of invariants. The three lowest ones write:

$$C_1 = \int_{x_{\min}}^{x_{\max}} u \, dx \,, \quad C_2 = \int_{x_{\min}}^{x_{\max}} u^2 \, dx \,, \quad C_3 = \int_{x_{\min}}^{x_{\max}} \left(u^3 - 3\beta(\partial_x u)^2\right) \, dx \,. \tag{4.1}$$

As a direct consequence of the weak formulation, the mass invariant $C_1$ is exactly preserved when using the spectral element schemes previously introduced. Indeed, when using a constant for test-function one obtains:

$$\int_{x_{\min}}^{x_{\max}} \partial_t u_h \, dx = -\int_{x_{\min}}^{x_{\max}} (u_h \partial_x u_h + \beta \partial_x f_h) \, dx$$

so that, since the SEM approximation of $\partial_x$ is exact for any polynomial of degree $N$ and since the GLL quadrature is exact for polynomials of degree $2N-1$

$$\frac{d}{dt}\left(\int_{x_{\min}}^{x_{\max}} u_h \, dx\right) = -\Big[\frac{u_h^2}{2} + \beta f_h\Big]_{x_{\min}}^{x_{\max}} = 0$$

by periodicity. Note that this holds with or without overintegration of the non-linear term. As a result, using any consistent approximation of the operator $\partial_t$ one obtains that $C_1$ is constant. Such a result is rather satisfactory, since many of the schemes described in the literature on the KdV equation do not show the same property.

The time discretization play a key role in the preservation of the energy invariant $C_2$. To ensure its conservation, a first possibility is to make use of a scheme especially designed to this end. An example of such a scheme is the standard Crank-Nicholson (CN) scheme. This approach is retained *e.g.* in the recent paper [40] where the CN scheme is used in conjunction with a specific Discontinuous Galerkin (DG) designed by tuning the DG parameters to preserve the two first invariants. With the space discretization proposed in this paper, the use of the CN scheme would lead to preservation of the two first invariants provided that (i) the quadrature associated to the non-linear term is exactly computed and if (ii) the third order term is treated

using the variant 2 of the SEM scheme. This is mainly a consequence of the fact that for CN:

$$\partial_t(u^2) = 2u\partial_t u \approx (u_{n+1} + u_n)\frac{u_{n+1} - u_n}{\tau} = \frac{1}{\tau}(u_{n+1}^2 - u_n^2)$$

where $u_n, u_{n+1}$ are the numerical solutions at time $t_n, t_{n+1}$, $\tau = t_{n+1} - t_n$ being the time step. Using this approach shows however two drawbacks: (i) loss of time accuracy, since the CN scheme is only second order accurate, and (ii) increase of the computational cost, since a non-linear solve is needed at each time-step. Going back to RK methods, it is known since [15] that a RK method preserves all quadratic invariants if and only if its coefficients satisfy $b_i a_{ij} + b_j a_{ji} = b_i b_j$ for all $1 \leqslant i, j \leqslant s$, see also *e.g.* [13, 22]. These conditions impose strong requirements on the coefficients and are satisfied only by some IRK methods. Nevertheless, even if ERK or IMEX RK cannot preserve all quadratic invariants, it is possible to focus on the preservation of a specific invariants and ensure it by projection at the end of each time step while preserving the accuracy of the overall scheme. Hereafter, two possibilities are discussed.

- A first possibility is to complete the IMEX RK scheme by a $L^2$ projection of the RK solution onto the hypersurface associated to the constraints. This can be achieved by introducing time dependent Lagrange multipliers. As shown in Section 5, the two first invariants can then be exactly preserved. Because one can derive an exact expression of the Lagrange multipliers the computational efficiency is maintained. Details on the implementation of this approach, and on the fact that the time accuracy is preserved, are provided in Appendix.
- A second possibility is to proceed by interpolation / extrapolation, at each time-step, of the solutions obtained by using two different RK schemes. One can also look at that as a non-orthogonal projection [7, 9, 10]. Then, since both schemes preserve the first invariant, it is only required to compute an interpolation / extrapolation time dependent factor that allows to preserve the second invariant. If we use such an approach, the computational cost is a priori twice greater, but this is no longer true with an embedded RK IMEX scheme. In this case, one only modifies the $b_i$ so that the $u_{n,i}$ are the same (see Section 2.1). Moreover, even if the embedded scheme is of order $q < p$, the accuracy may be preserved, see Appendix and [9]. For instance, from ARS(2,3,3) one obtains a lower order scheme simply by modifying the last line of Table 2.1. Because for consistency reason the sum of these coefficients should equal 1, in Section 5 we simply use the pair $\{1/4, 3/4\}$ instead of $\{1/2, 1/2\}$, for both the ERK and the DIRK parts, which yields a first order IMEX scheme. Details are also given in Appendix.

These two approaches are numerically compared in Section 5.2.

## 5. Numerical experiments.

**5.1. Test-case 1:.** Like in [42], we consider the KdV equation with $\beta = 0.022^2$ in the periodic domain $(0, 2)$ and assume the initial condition $u_0 = \cos(\pi x)$. Fig. 5.1 shows the expected solution at different times, as computed with $K = 40$ elements and a polynomial approximation degree $N = 5$. The third order derivative is approximated on the basis of the *variant 1*, see Section 2.2. Exact integration of the non-linear term is achieved by using the GLL grid associated to the polynomial approximation degree $M = 8 \geq 3N/2$, see Section 3.

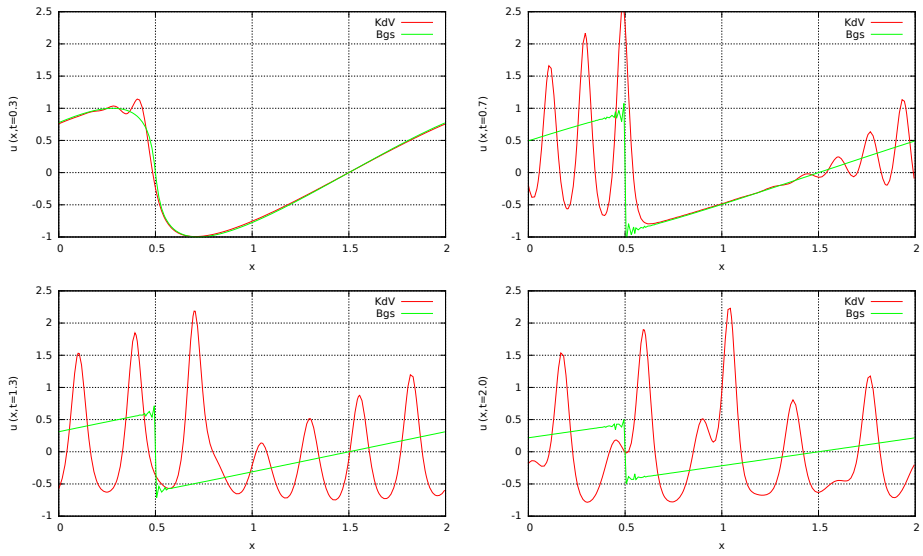


FIG. 5.1. *Test-case 1: Solution of the KdV and Burgers equations at times* $t = \{0.3, 0.7, 1.3, 2\}$. *Computation done with* $K = 40$ *elements and a polynomial degree* $N = 5$.

We have also plotted in Fig. 5.1 the result obtained for the Burgers equation, using the conservative form of the transport term, $\partial_x(u^2/2)$, rather than the convective one, $u\partial_x u$. Because the Burgers solution develops a shock, overintegration is not sufficient and so the SVV stabilization is mandatory. We have used the control parameters $m_N = [\sqrt{N}] = 2$ (with [.] for nearest integer) and $\epsilon_N = h/N$, where $h = (x_{\max} - x_{\min})/K$ is the element size. As expected, the Burgers solution shows tiny oscillations at the shock, which is not surprising since this linear stabilization is not sufficient to smooth all oscillations, contrarily, *e.g.*, to the non-linear entropy viscosity method [19].

The two following examples are considered as standard benchmarks for KdV solvers, see [18] or *e.g.* [1, 12, 38, 43] when using the FEM.

**5.2. Test-case 2.** This example describes the interaction between two solitons. Because an exact solution is known for the open domain $\Omega \equiv \mathbb{R}$, it allows to carry out an accuracy study.

As described *e.g.* in [18], for $\beta = 4.84\,10^{-4}$ the following analytic expression solves the KdV equation:

$$u_{ex}(x,t) = 12\beta(LogF)_{xx}\,, \text{with}\, F = 1 + e^{\eta_1} + e^{\eta_2} + \alpha e^{(\eta_1+\eta_2)}\,,\ \eta_i = \alpha_i x - \alpha_i^3\beta t + b_i\,,$$
$$\alpha = \left(\frac{\alpha_1 - \alpha_2}{\alpha_1 + \alpha_2}\right)^2\,,\ \alpha_1 = \sqrt{0.3/\alpha}\,,\ \alpha_2 = \sqrt{0.1/\alpha}\,,\ b_1 = -0.48\alpha_1\,,\ b_2 = -1.07\alpha_2\,.$$

Computations have been carried out for $x \in (-1, 4)$ and $t \in (0, 6.3)$, assuming again periodicity and using for initial condition the exact value at $t = 0$. Two different globally third order accurate IMEX schemes have been used: ARS(3,4,3) and ARS (2,3,3) [3], with quite similar results. The results that we present hereafter are those obtained with ARS (2,3,3). In the considered time interval, on an animation one clearly observes the propagation of the two solitons of magnitude 0.9 and 0.3, their crossing and then their reformation.

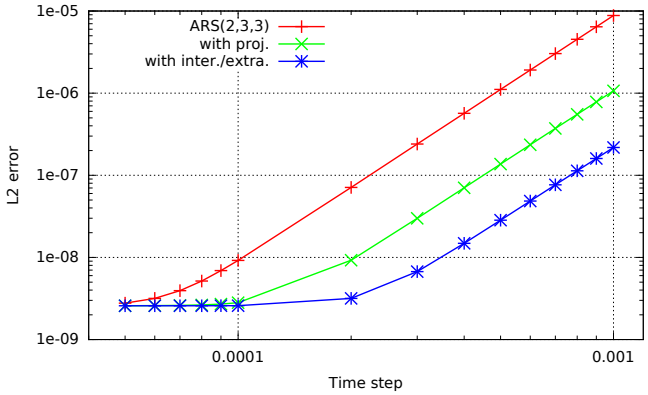


FIG. 5.2. *Test-case 2: Time accuracy for the ARS(2,3,3) scheme, in its basic version and when associated to an additional correcting step.*

We first check if the third order time accuracy of the RK IMEX scheme is obtained. To this end, computations have been carried out with the fine grid obtained for $K = 300$ and $N = 5$, using different time-steps. Moreover, in Section 4 it is claimed that the accuracy of the IMEX scheme is preserved when completing it with an additional step, in view of preserving the two first invariants. To check that, computations have also been carried out using (i) the projection and the (ii) interpolation/extrapolation techniques. Results are provided in Fig. 5.2. Clearly, ARS(2,3,3) is third order accurate, even if associated with an additional correcting step. In the present example, it turns out that the accuracy is improved when using a correcting step, and that the best accuracy is obtained with the interpolation/extrapolation technique. This is the approach used to check the space accuracy.

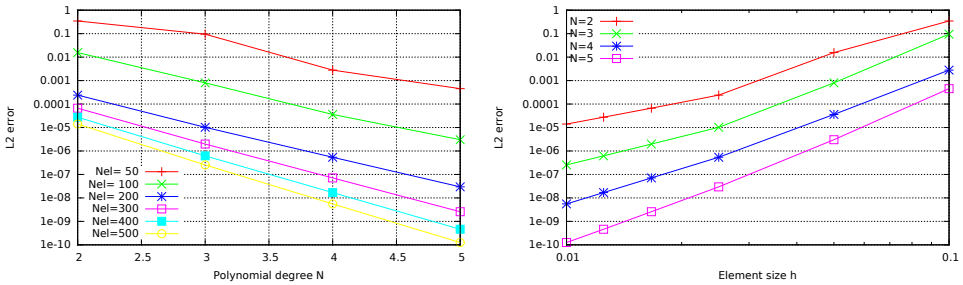


FIG. 5.3. *Test-case 2: $L^2$-error with respect to the polynomial degree $N$ (at left) and to the element size $h$ (at right)*

To carry out the space accuracy study, we have considered polynomial approximation degrees such that $2 \leq N \leq 5$ and the following numbers of elements, $K = \{50, 100, 200, 300, 400, 500\}$. To make negligible the time-stepping error, we have used the small time-step value $\tau = 5\,10^{-5}$. Fig. 5.3 shows the $L^2$ norm of the gap between the numerical and exact solutions. As expected, one clearly observes, in Fig. 5.3(left) the exponentially fast decrease of the error with respect to the polynomial degree $N$ and in Fig. 5.3(right) an algebraic convergence with respect to the element size $h$ of order about $N + 1$, which is optimal. It should however be mentioned that:

- Such accuracy results cannot be obtained for $\Omega = (0, 4)$, as considered in [1, 18, 43]. In these papers, the listed errors remain indeed greater than the value of $u_{ex}(0, 0)$, *i.e.*, around $10^{-6}$. As a result, when using this computational domain one observes a saturation in the decrease of the error. The phenomenon is overcome when using $\Omega = (-1, 4)$, because at both end sides of $\Omega$, $u_{ex}$ is then smaller than the truncation error.

- To avoid an artifact due to a superconvergence associated to the quadrature rule, the $L^2$ errors have been computed by using here again the overintegration technique, *i.e.* in each elements the GLL points obtained for $N = 8$ have been used as quadrature points. Some convergence rates of Fig. 5.3 may even seem greater than $N + 1$ ! This is due to the fact that for too rough discretizations, *e.g.*, $N = 2$ and $K \leq 200$, the asymptotic regime is not yet reached. We are here in the underresolved case considered in Section 5.4.

**5.3. Test-case 3.** Starting from a Gaussian as initial condition, interesting solutions may be obtained. They crucially depend on the value of the $\beta$ parameter with respect to a critical value $\beta_c$. For $\beta \ll \beta_c$, the initial condition splits into a series of stiff solitons, which number depends on the value of $\beta$. We use this example to show that even for very stiff solutions, the high order approximation may yield satisfactory results. Moreover, as *e.g.* in [18], we check on this example the conservation of the 3 lowest invariants, see equation (4.1).

As in [18, 43] we solve the KdV equation for $t \in (0, 12.5)$ and in the computational domain $\Omega = (-15, 15)$. For initial condition we use $u(x, 0) = \exp(-x^2)$, so that the critical $\beta$ is $\beta_c = 0.0625$ [5]. We choose the value $\beta = 10^{-3} \ll \beta_c$, so that one expects the formation of 9 solitons, in agreement with the formula $N_{soliton} = \lfloor (13\beta)^{-0.5} \rfloor$ ($\lfloor . \rfloor$ for integer part) [26].

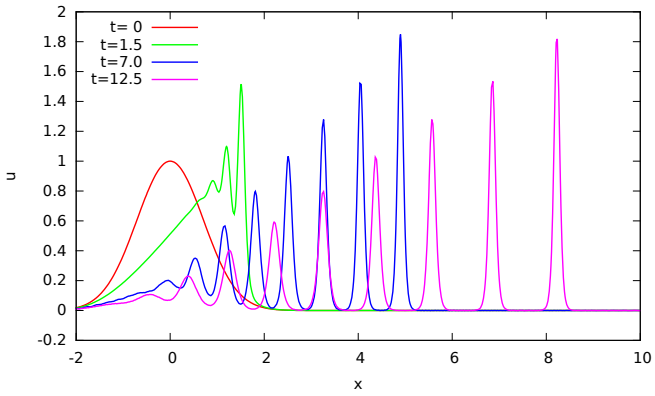


FIG. 5.4. *Test-case 3: Solution at different times.*

Computations have been carried out using $K = 240$ and $K = 300$ elements, with a polynomial degree $N = 5$. In terms of number of grid-points, $K = 240$ and $K = 300$ correspond to the values $d = 1200$ and $d = 1500$ used in [18] and in [43], respectively. The solution obtained at different times, without correcting step and for $K = 300$, is shown in Fig. 5.4. After the splitting into solitons one can check that the propagation velocity $V$ of each soliton is proportional to its amplitude $A$, since the maxima are aligned on a straight line, and that as theoretically predicted $V = A/3$ [5].

In Tables 5.1 and 5.2, we provide the invariants at several times, as obtained

| Time | 0.0 | 2.5 | 5.0 | 7.5 | 10.0 | 12.5 |
|---|---|---|---|---|---|---|
| $C_1$ | 1.77245 | 1.77245 | 1.77245 | 1.77245 | 1.77245 | 1.77245 |
| $C_2$ | 1.25331 | 1.25325 | 1.25231 | 1.25136 | 1.25174 | 1.25179 |
| $C_3$ | 1.01957 | 1.01898 | 1.00940 | 1.00253 | 1.01040 | 1.01463 |

TABLE 5.1
*Test-case 3: The invariant $C_1$, $C_2$ and $C_3$ at different times, $K = 240$ and $N = 5$.*

with $K = 240$ and $K = 300$ elements, respectively. As expected, one can check that invariant $C_1$ is perfectly conserved. Concerning the two other invariants, for $K = 240$, at the final time $t = 12.5$ the relative variations of the coefficients $C_2$ and $C_3$ are of $-0.12\,\%$ and $-0.48\,\%$, respectively. Of course, better results are obtained with $K = 300$ elements, with relative variations for $C_2$ and $C_3$ of $-0.04\,\%$ and $-0.13\,\%$.

| Time | 0.0 | 2.5 | 5.0 | 7.5 | 10.0 | 12.5 |
|---|---|---|---|---|---|---|
| $C_1$ | 1.77245 | 1.77245 | 1.77245 | 1.77245 | 1.77245 | 1.77245 |
| $C_2$ | 1.25331 | 1.25330 | 1.25335 | 1.25317 | 1.25283 | 1.25279 |
| $C_3$ | 1.01957 | 1.01948 | 1.01912 | 1.01888 | 1.01864 | 1.01829 |

TABLE 5.2
*Test-case 3: The invariant $C_1$, $C_2$ and $C_3$ at different times, $K = 300$ and $N = 5$.*

The latter results can be compared to those in [43], obtained with a *quintic B-spline* FEM. With the same number of grid-points, the relative variations for $C_1$, $C_2$ and $C_3$ of $+0.05\,\%$, $+0.016\,\%$ and $+0.35\,\%$.

As explained in Section 2.1, the conservation of the two first invariants can be obtained using an additional correcting step, based on a projection on the manifold described by the two first invariants or by interpolation/extrapolation of two embedded RK IMEX schemes. The results obtained with $N = 5$ and $K = 240$ elements when using the two techniques are provided in Table 5.3.

| Time | 0.0 | 2.5 | 5.0 | 7.5 | 10.0 | 12.5 |
|---|---|---|---|---|---|---|
| $C_1$ | 1.77245 | 1.77245 | 1.77245 | 1.77245 | 1.77245 | 1.77245 |
| $C_2$ | 1.25331 | 1.25331 | 1.25331 | 1.25331 | 1.25331 | 1.25331 |
| $C_3$ (1) | 1.01957 | 1.01907 | 1.01068 | 1.00415 | 1.01051 | 1.01660 |
| $C_3$ (2) | 1.01957 | 1.01910 | 1.01054 | 1.00250 | 1.00871 | 1.01662 |

TABLE 5.3
*Test-case 3: The invariant $C_1$, $C_2$ and $C_3$ at different times, $K = 240$ and $N = 5$, SEM scheme completed with (1) a projection step and (2) an interpolation/extrapolation step.*

**5.4. Underresolved test-case 3.** The numerical results presented till now have been obtained using the *variant 1* of the SEM scheme for the third order derivative and overintegration for stabilization, but very close results can be obtained when using the *variant 2* of the scheme, the SVV method for stabilization or even without numerical stabilization. To make comparisons between these different approaches, we consider here again the test-case 3 but with a cruder mesh, *i.e.* $K = 180$ elements, again with a polynomial degree $N = 5$.

In the Fig. 5.5 we compare the results obtained, at the final time $t = 12.5$ and when using the *variant 1* of the SEM scheme, (i) without stabilization, (ii) with overintegration of the non-linear term ($M = 8$) or (iii) using the SVV method, with

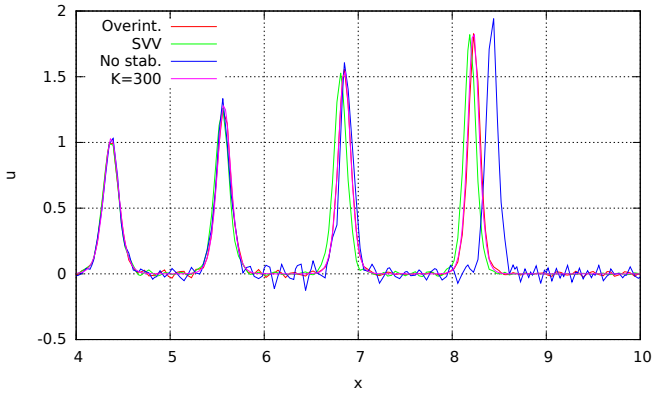


FIG. 5.5. *Test-case 3: Underresolved solutions at time* $t = 12.5$ *using different stabilizations: overintegration, SVV and no-stabilization.*

again $m_N = [\sqrt{N}] = 2$ and $\epsilon_N = h/N$. For the sake of comparison, the solution obtained with $K = 300$ elements is also shown. Clearly, if no stabilization is used, then the solution shows oscillations and moreover the propagation velocities of the solitons are overvalued. The best result is here obtained with the overintegration of the non-linear term: The solution is indeed smoother and the propagation velocities are not affected. One remarks that the SVV method slightly affects the propagation velocity. This phenomenon is strongly amplified when choosing $m_N = 0$, *i.e.* when also inserting viscosity on the low frequencies of the solution.

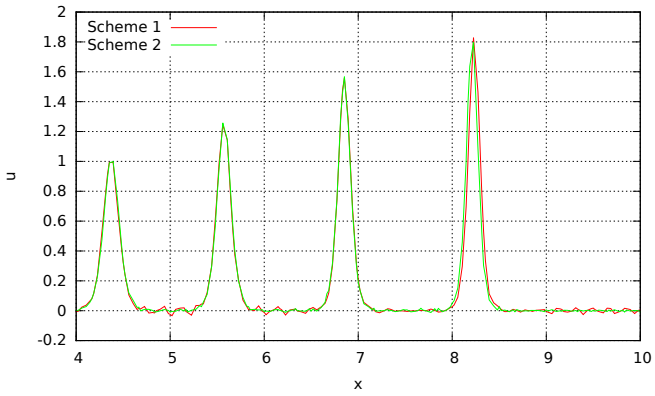


FIG. 5.6. *Test-case 3: Underresolved solutions* $t = 12.5$ *with the two variants of the SEM scheme.*

In the Fig. 5.6, we compare the two variants of the SEM scheme. Here one may observe that the propagation velocities are not affected, but that *variant 2* is qualitatively better than *variant 1* since providing the smoother solution.

**6. Concluding remarks.** Standard SEM schemes, *i.e.* involving high order $C^0$ continuous elements, have been proposed to address the approximation of the KdV equation. These schemes are mainly based on a special way to approximate the third order derivative term and it has been shown that an exact integration of the non-linear transport term was of interest. Optimal accuracy results have been obtained using

this methodology. Taking advantage of the fact that the SEM matrix is diagonal, the present SEM schemes do not suffer from an increase of the number of unknowns. Because the algorithms make use of $C^0$ continuous elements, the implementation is simple and can be easily extended to multidimensional geometries. It has also been shown that preserving the two first invariants was possible, *e.g.* by looking at them as constraints and introducing Lagrange multipliers or by using an interpolation / extrapolation technique between two embedded RK IMEX schemes. Beyond the KdV equation, the present SEM methodology can *a priori* apply to other PDEs showing higher order derivative terms.

**Appendix.** The two approaches described hereafter are valid for any RK schemes, are not specific to the KdV equation and are not restricted to one dimensional problems. We however focus on the preservation of specific linear and quadratic invariants.

**.1. Invariants preservation by projection.** At each time step, we proceed by discrete $L^2$ projection of the IMEX solution onto the manifold associated to the discrete versions of the two first invariants. Starting from the discrete solution $u_h(x,t_n)$ at time $t_n$, we first compute the grid-point values $y_i$ using the RK scheme and then define $u_h(x,t_{n+1})$ by orthogonal projection.

Denoting $w_i$ the quadrature coefficient associated to the grid-points $x_i$, $1 \leq i \leq d$, we define $C_1 = \sum_i w_i u_h(x_i,t_n)$ and $C_2 = \sum_i w_i (u_h(x_i,t_n))^2$. The optimization problem then writes: Find the $\delta y_i$ that minimize the functional $F(\delta y_1, \cdots, \delta y_d) = \sum_i w_i \delta y_i^2$, such that $\sum_i w_i(y_i+\delta y_i) = C_1$ and $\sum_i w_i (y_i+\delta y_i)^2 = C_2$. The discrete solution at time $t_{n+1}$ is then set as $u_h(x_i,t_{n+1}) \equiv u_i = y_i + \delta y_i$.

To transform the constrained optimization problem into a non constrained one, we introduce the functional:

$$L(\delta y_1, \cdots, \delta y_d, \lambda_1, \lambda_2) = \sum_i w_i \delta y_i^2 + \lambda_1 \Big( \sum_i w_i (y_i+\delta y_i) - C_1 \Big) + \lambda_2 \Big( \sum_i w_i (y_i+\delta y_i)^2 - C_2 \Big)$$

and the problem is now to find the $\delta y_i$ together with the Lagrange multipliers $\lambda_1$ and $\lambda_2$. At the optimum of this saddle point problem, the gradient of the functional vanishes. This yields:

$$\partial_{\delta y_i} L = 2 w_i \delta y_i + \lambda_1 w_i + 2\lambda_2 w_i (y_i + \delta y_i) = 0 \tag{.1}$$

$$\partial_{\lambda_1} L = \sum_i w_i (y_i + \delta y_i) - C_1 = 0 \tag{.2}$$

$$\partial_{\lambda_2} L = \sum_i w_i (y_i + \delta y_i)^2 - C_2 = 0 \tag{.3}$$

so that, from (.1)

$$\delta y_i = -\frac{\lambda_2}{1+\lambda_2} y_i - \frac{\lambda_1}{2(1+\lambda_2)} \quad \text{and} \quad u_i = \frac{1}{1+\lambda_2} y_i - \frac{\lambda_1}{2(1+\lambda_2)} \,. \tag{.4}$$

It remains to plug the last expression in (.2) and (.3). Using the notation $S_y = \sum_i w_i y_i$, $S_{y^2} = \sum_i w_i y_i^2$ and $S_1 = \sum_i w_i = x_{\max} - x_{\min}$, one obtains:

$$S_y - S_1 \frac{\lambda_1}{2} - C_1(1+\lambda_2) = 0 \tag{.5}$$

$$S_{y^2} - S_y \lambda_1 + S_1 \frac{\lambda_1^2}{4} - C_2 (1+\lambda_2)^2 = 0$$

This non-linear system in $\lambda_1$ and $\lambda_2$ can be easily solved. With $(1+\lambda_2)$ from (.5), one obtains that $\lambda_1$ solves:

$$\frac{1}{4}(S_1^2 - \alpha S_1)\lambda_1^2 - (S_1 S_y + \alpha S_y)\lambda_1 + S_y^2 - \alpha S_{y^2} = 0 \tag{.6}$$

where $\alpha = C_1^2/C_2 > 0$. One can compute $\lambda_1$ from this equation and then obtain $\lambda_2$ from (.5). Note that since $\alpha \approx S_y^2/S_{y^2}$, the negative discriminant is relevant, because in case of equality this yields $\lambda_1 = 0$. Once knowing the Lagrange multipliers, from (.4) one computes the $u_i$.

Now we show that the approximation order of the RK scheme is preserved. Assuming we use a RK scheme of order $p$ ($p = 3$ in our examples) to compute the $y_i$, $1 \le i \le d$, then the local truncation error, *i.e.* the gap between the $y_i$ and the exact solution obtained at time $t_{n+1}$ starting from $u_h(x, t_n)$, is $O(\tau^{p+1})$. We can readily deduce that $C_1 - S_y$ and $C_2 - S_{y^2}$ are also $O(\tau^{p+1})$. Next we obtain that

$$S_1^2 - \alpha S_1 = O(1), \quad S_1 S_y + \alpha S_y = O(1) \quad \text{and} \quad S_y^2 - \alpha S_{y^2} = O(\tau^{p+1}).$$

Equation (.6) then shows that $\lambda_1$ is $O(\tau^{p+1})$ and we deduce from equation (.5) that $\lambda_2$ is also $O(\tau^{p+1})$. Taking into account the fact that $|\lambda_1|, |\lambda_2| \ll 1$, from (.4) one has:

$$\delta y_i \approx -\lambda_2 y_i - \frac{\lambda_1}{2}$$

so that the correction behaves like the Lagrange multipliers. As a result, the correction by the $\delta y_i$ is consistent with the accuracy of the RK scheme.

It should be noticed that more than two invariants can be considered, but certainly at the price of a non-explicit formulation of the Lagrange multipliers.

**.2. Invariants preservation by interpolation / extrapolation.** Here we assume to have at hand two RK IMEX schemes. Knowing the numerical solution at time $t_n$, $u_h(x, t_n)$, we compute the grid-point values $y_i$ and $z_i$, $1 \le i \le d$, at time $t_{n+1}$ with the two RK IMEX schemes. Because each scheme preserves the invariant $C_1$, any linear combination of the two solutions will be $C_1$-invariant. The goal is then to define an interpolation / extrapolation factor $\lambda$, such that $C_2$ is preserved. Thus, at time $t_{n+1}$, we define

$$u_i = (1-\lambda)y_i + \lambda z_i\,, \quad \sum_i w_i u_i^2 = C_2$$

where again $C_2 = \sum_i w_i (u_h(x_i, t_n))^2$, and $w_i$ are the quadrature coefficient associated to the grid-points $x_i$.

Using notations similar to those previously introduced, one easily checks that $\lambda$ should solve:

$$S_{(z-y)^2}\lambda^2 + 2S_{y(z-y)}\lambda + S_{y^2} - C_2 = 0\,. \tag{.7}$$

The (reduced) discriminant writes, $\Delta = S_{y(z-y)}^2 + S_{(z-y)^2}(C_2 - S_{y^2})$. It is positive as soon as $C_2 \ge S_{y^2}$, *i.e.* if the $y$-scheme is dissipative. In case of equality, the coefficient $\lambda$ should vanishes, which means that the relevant solution is obtained by using against the discriminant the sign of the quantity $S_{y(z-y)}$.

Let us now assume that the $y$ scheme is of order $p$ and the $z$-scheme of order $q < p$. By definition, for any grid-point we can write

$$y_i = \bar{u}_i + O(\tau^{p+1}), \quad z_i = \bar{u}_i + \psi_i \tau^{q+1} + O(\tau^{q+2}),$$

where $\bar{u}_i$ is the exact solution, obtained at point $x_i$ and time $t_{n+1}$, when starting from $u_h(x, t_n)$. Hence, coming back to the coefficients of equation (.7) we have

$$S_{(z-y)^2} = O(\tau^{2q+2}), \quad S_{y(z-y)} = S_{\bar{u}\psi}\tau^{q+1} + O(\tau^{q+2}), \quad S_{y^2} - C_2 = O(\tau^{p+1}).$$

If we assume that $S_{\bar{u}\psi} \neq 0$, then the discriminant of (.7) is positive, at least for $\tau$ small enough, and we obtain that $\lambda$ is $O(\tau^{p-q})$. Hence, the accuracy of the $y$-scheme is preserved. A similar result was previously provided for ERK schemes in [9, Theorem 3.1].

## REFERENCES


[1] E.N. Aksan, A. Özdes, Numerical solution of the Korteweg-de Vries equation by Galerkin B-spline finite element method, *Appl. Math. Comput.* 175 (2006) 1256-1265.

[2] U.M. Ascher, S.J. Ruth, B. Wetton, Implicit-explicit methods for time-dependent PDE's, *SIAM J. Numer. Anal.* 32 (1995) 797-823.

[3] U.M. Ascher, S.J. Ruth, R.J. Spiteri, Implicit-explicit Runge-Kutta methods for time-dependent partial differential equations, *Appl. Num. Math.* 25 (1997) 151-167.

[4] G.A. Baker, V.A. Dougalis, O.A. Karakashian, Convergence of Galerkin Approximations for the Korteweg-de Vries equation, *Mathematics of Computation* 40 (163) (1983) 419–433.

[5] Y.U. Berezin, V.I. Karpman, Nonlinear evolution of disturbances in plasmas and other dispersive media, *Soviet Physics Jetp* 24 (5) (1967) 1049-1055.

[6] J.L. Bona, V.A. Dougalis, O.A. Karakashian, Fully discrete galerkin methods for the Korteweg-de Vries equation, *Comp. & Maths. with Appls.* 12A (7) (1986) 859-884.

[7] N.D. Bueno, C. Mastroserio, Explicit methods based on a class of four stage fourth order Runge-Kutta methods for preserving quadratic invariants, *J. of Comput. and Appl. Math.* 20 (1996) 247-260.

[8] J.C. Butcher, A histoty of Runge-Kutta methods, *Appl. Num. Math.* 25 (1997) 151-167.

[9] M. Calvo, D. Hernández-Abreu, J.I. Montijano, L. Rández, On the preservation of invariants by explicit Runge-Kutta methods, *SIAM J. Sci. Comput.* 28(3) (2006), 868885.

[10] M. Calvo, M. P. Laburta, J.I. Montijano, L. Rández, Runge-Kutta projection methods with low dispersion and dissipation errors, *Adv Comput Math* 41 (2015) 231251.

[11] C. Canuto, M. Hussaini, A. Quarteroni, T. Zang, *Spectral Methods, Evolution to Complex Geometries and Applications to Fluid Dynamics*, Springer Verlag, 2007.

[12] G.F. Carey, Y. Shen, Approximation of the KdV equation by least square finite elements, *J. Comput. Methods in Appl. Mech. and Engrg.* 93 (1991) 1-11.

[13] E. Celledoni, R.I. McLachlan, D.I. McLaren, B. Owen, G.R.W. Quispel, W.M. Wright, Energy-preserving Runge-Kutta methods, *ESAIM: M2AN* 43 (2009) 645-649.

[14] G. Cohen, P. Monk, Gauss point mass lumping schemes for Maxwell's equations, *Numer. Methods Partial Differential Equations*, 14 (1998), 63-88.

[15] G.J. Cooper, Stability of runge-kutta methods for trajectory problems *IMA Journal of Numerical Analysis*, Volume 7(1) (1987), 1-13.

[16] M.O. Deville, P.F. Fischer, E.H. Mund, *High-order methods for incompressible fluid flow*, Cambridge University Press, New York, 2002.

[17] D. Dutykh, T. Katsaounis, D. Mitsotakis, Finite volume methods for unidirectional dispersive wave models, *Int. J. for Numerical Methods in Fluids*, 71 (2013) 717-736.

[18] L.R.T. Gardner, G.A. Gardner, A.H.A. Ali, Simulations of solitons using quadratic spline finite elements, *J. Comput. Methods in Appl. Mech. and Engrg.* 92 (1991) 231-243.

[19] J.L. Guermond, R. Pasquetti, B. Popov, Entropy viscosity method for non-linear conservation laws, *J. Comput. Phys.* 230 (11) (2011) 4248-4267.

[20] H. Holden, K.H. Karlsen, N.H. Risebro, Operator splitting methods for generalized Korteweg-de Vries equations, *J. Comput. Phys.* 153 (1999) 203-222.

[21] T.J.R. Hugues, G.R. Feijoo, L. Mazzei, J.B. Quincy, The variational multiscale method - a paradigm for computational mechanics, *Comput. Methods in Appl. Mech. Engrg.* 166 (1998) 3-24.

[22] A. Iserles, A. Zanna, Preserving algebraic invariants with Runge-Kutta methods, *J. of Comput. and Appl. Math.* 125 (2000) 69-81.

[23] T. Kappeler, P. Topalov, Global wellposedness of KdV in $H^{-1}(\mathbb{T}, \mathbb{R})$, *Duke Mathematical J.* 135 (2006) 327-360.

[24] G.E. Karniadakis, S.J. Sherwin, *Spectral hp element methods for CFD*, Oxford Univ. Press, London, 1999.

[25] R.M. Kirby, G.E. Karniadakis, De-aliasing on non uniform grids: algorithms and applications, *J. Comput. Phys.* 191 (2003) 249-264.

[26] V.I. Karpman, An asymptotic solution of the Korteweg-de Vries equation, *Physics Letters* 25A (10) (1967) 708-709.

[27] P.D. Lax, C.D. Levermore, The small dispersion limit of the Korteweg-de Vries equation. I, *Comm. on Pure and Appl. Math.* XXXVI (1983) 253-290.

[28] Y. Maday, A.T. Patera, Spectral element methods for the incompressible Navier-Stokes equations, in A.K. Noor (Editor), State-of-the-Art Surveys in Computational Mechanics, ASME, New York, 1989, 71-143.

[29] Y. Maday, S.M.O. Kaber, E. Tadmor, Legendre pseudo-spectral viscosity method for nonlinear conservation laws, *SIAM J. Numer. Anal.* 30 (2) (1993) 321-342.

[30] J.W. Miles, The Korteweg-de Vries equation: a historical essay, *J. Fluid Mech.* 106 (1984) 131-147.

[31] J.P. Ohlsson, P. Schlatter, P.F. Fischer, D.S. Henningson, Stabilization of the spectral element method in turbulent flow simulations, in *Lecture Notes in Computational Science and Engineering* 76, Springer-Verlag Berlin Heidelberg 2011, 449-458.

[32] L. Pareschi, G. Russo, Implicit-Explicit Runge-Kutta schemes for stiff systems of differential equations, Recent trends in numerical analysis, 269-288, Nova Science Publishers, Inc. Commack, NY, USA 2000.

[33] A.T. Patera, A spectral element method for fluid dynamics: laminar flow in a channel expansion, *J. Comput. Phys.* 54 (1984) 468-488.

[34] J.M. Sanz-Serna, I. Christie, Petrov-Galerkin Methods for Nonlinear Dispersive Waves, *J. Comput. Phys.* 39 (1981) 94-102.

[35] J.M. Sanz-Serna, An explicit finite-difference scheme with exact conservation properties, *J. Comput. Phys.* 47 (1982) 199-210.

[36] J. Shen, A new dual-Petrov-Galerkin method for third and higher odd-order differential equations: Application to the KdV equation, *SIAM J. Numer. Anal.* 41 (5) (2003) 1595-1619.

[37] E. Tadmor, Convergence of spectral methods for nonlinear conservation laws, *SIAM J. Numer. Anal.* 26 (1) (1989) 30-44.

[38] T.R. Taha, M.J. Ablowitz, Analytical and numerical aspects of certain nonlinear evolution equations. III. Numerical, Korteweg-de Vries equation, *J. Comput. Phys.* 55 (1984) 231-253.

[39] C.J. Xu, R. Pasquetti, Stabilized spectral element computations of high Reynolds number incompressible flows, *J. Comput. Phys.* 196 (2) (2004) 680-704.

[40] N. Yi, Y. Huang, H. Liu, A direct discontinuous Galerkin method for the generalized Korteweg-de Vries equation: Energy conservation and boundary effect. *J. Comput. Phys.* 242 (2013) 351-366.

[41] R. Winther, A conservative finite element method for the Korteweg-de Vries equation, *Mathematics of computation*, 34 (149) (1980) 23-43.

[42] N.J. Zabusky, M.D. Kruskal, Interaction of solitons in a collisionless plasma and the recurence of initial states, *Phys. Rev. Letters* 15 (6) (1965) 240-243.

[43] S.I. Zaki, A quintic B-spline finite elements scheme for the KdVB equation, *J. Comput. Methods in Appl. Mech. and Engrg.* 188 (2000) 121-134.